pert consensus ocument Reportin chec list for uantification of pulmonary con estion y lun ultrasoun in heart failure

CSPG4-specific CAR.CIK lymphocytes as a novel therapy for the treatment of multiple soft tissue sarcoma histotypes

Valeria Leuci[1-2], Chiara Donini[1-2]*, Giovanni Grignani[1], Ramona Rotolo[1], Giulia Mesiano[1-2], Erika Fiorino[1-2], Loretta Gammaitoni[1], Lorenzo D'Ambrosio[1], Alessandra Merlini[1-2], Elisa Landoni[4], Enzo Medico[1-2], Sonia Capellero[1-2], Lidia Giraudo[1], Giulia Cattaneo[1-2], Ilenia Iaia[1-2], Ymera Pignochino[1-2], Marco Basiricò[1-2], Elisa Vigna[1-2], Alberto Pisacane[1], Franca Fagioli[3], Soldano Ferrone[5], Massimo Aglietta[1-2], Gianpietro Dotti[4-6], Dario Sangiolo[1-2]*

[1] Candiolo Cancer Institute, FPO-IRCCS. Candiolo, Italy.

[2] Department of Oncology, University of Torino, Italy

[3] Pediatric Onco-Hematology, Stem Cell Transplantation and Cellular Therapy Division, Regina Margherita Children's Hospital, University of Turin, Italy

[4] Lineberger Comprehensive Cancer Center, University of North Carolina at Chapel Hill, Chapel Hill, North Carolina, USA.

[5] Division of Surgical Oncology, Department of Surgery, Massachusetts General Hospital, Harvard Medical School, Boston, MA, USA.

[6] Department of Microbiology and Immunology, University of North Carolina, Chapel Hill, North Carolina, USA

* *VL and CD equally contributed to this study*

Running header: CSPG4 CAR.CIK effectively eradicate soft tissue sarcomas.

Keywords: CIK lymphocytes, Chimeric Antigen Receptor (CAR), Soft Tissue Sarcomas, Adoptive Immunotherapy, CSPG4.

Financial support: This study was supported by fundings from: "Associazione Italiana Ricerca sul Cancro" (AIRC) IG-2017 n. 20259 (DS), IG-2019 n. 23104 (GG); Ricerca corrente Progetto CAR-T RCR-2019-23669115 (DS, EM); FPRC ONLUS 5 × 1000, Ministero della Salute 2015 Cancer ImGen (DS, GG; EM); FPRC ONLUS 5X1000 MIUR 2014 (GG, LDA); Ministero della Salute (GR-2011-02349197) (DS), University of Torino Fondo Ricerca Locale 2017 (DS); Ricerca Corrente Ministero Salute 2020; Fondazione per la ricerca sui tumori dell'apparato muscoloscheletrico e rari Onlus CRT RF = 2016–0917 (GG). SF was supported by NIH grants R01DE028172 and R03CA216114 and by DOD grant W81XWH-16-1-0500. VL has received a fellowship from the Fondazione Nicola Ferrari ONLUS; MB has received a fellowship from ADISCO ONLUS.

Correspondence should be addressed to:

Dario Sangiolo, MD, PhD.
Division of Medical Oncology - Laboratory of Experimental Cell Therapy, Candiolo Cancer Institute, FPO - IRCCS, Provinciale 142 - 10060 Candiolo, Torino Italy.
Phone: +390119933503
Fax: +390119933522
e-mail: dario.sangiolo@ircc.it

Conflict of interest disclosure: G.D. and S.F. hold a patent on the CSPG4-CAR. G.D. has sponsor research agreements with Bluebird Bio, Cell Medica and Bellicum Pharmaceutical. G.D. serves in the scientific advisory board of MolMed S.p.A and Bellicum Pharmaceutical. The other authors declare no competing financial interests.

Word count: 5170

Total Figures: 6

Translational Relevance.

Our study has shown that cytokine-Induced killer lymphocytes (CIK) engineered with a CSPG4-CAR are effective in eliminating many types of soft tissue sarcoma (STS)-derived cells both *in vitro* and in immune deficient mice. These pre-clinical results provide a strong rationale for the clinical translation of the CSPG4-CAR.CIK-based immunotherapeutic strategy we have developed. Patients with unresectable high-grade STS who respond poorly to checkpoint inhibitor-based immunotherapy may greatly benefit from this novel immunotherapy.

Abstract

Purpose.

No effective therapy is available for unresectable soft tissue sarcomas (STS). This unmet clinical need has prompted us to test whether chondroitin sulfate proteoglycan 4 (CSPG4)-specific CAR-redirected cytokine-induced killer lymphocytes (CAR.CIK) are effective in eliminating tumor cells derived from multiple STS histotypes *in vitro* and in immunodeficient mice.

Experimental Design.

The experimental platform included patient-derived CAR.CIK and cell lines established from multiple STS histotypes. CAR.CIK were transduced with a retroviral vector encoding 2nd-generation CSPG4-specific CAR (CSPG4-CAR) with 4-1BB co-stimulation. The functional activity of CSPG4-CAR.CIK was explored *in vitro*, in 2D and 3D STS cultures, and in three *in vivo* STS xenograft models.

Results.

CSPG4-CAR.CIK were efficiently generated from STS patients. CSPG4 was highly expressed in multiple STS histotypes by *in silico* analysis and on all the 16 STS cell lines tested by flow cytometry. CSPG4-CAR.CIK displayed superior *in vitro* cytolytic activity against multiple STS histotypes as compared to paired unmodified control CIK. CSPG4-CAR.CIK also showed strong anti-tumor activity against STS spheroids; this effect was associated with tumor recruitment, infiltration, and matrix penetration. CSPG4-CAR.CIK significantly delayed or reversed tumor growth *in vivo* in three STS xenograft models (Leiomyosarcoma, UPS and Fibrosarcoma). Tumor growth inhibition persisted for up to 2 weeks following the last administration of CSPG4-CAR.CIK.

Conclusions.

This study has shown that CSPG4-specific CAR-redirected CIK effectively target multiple STS histotypes *in vitro* and in immunodeficient mice. These results provide a strong rationale to translate the novel strategy we have developed in to a clinical setting.

Introduction

Soft tissue sarcomas (STS) are rare tumors of mesenchymal origin that affect both children and adults (1). These peculiar tumors encompasses multiple histotypes, which are characterized by extremely variable biological and clinical behaviours. Chemotherapy and molecularly targeted approaches may offer transient disease control to patients non-eligible for radical surgical resection. However, the overall prognosis remains dismal with a 5-year survival rate of less than 25% (1-3). STS are also poorly responsive to checkpoint blockade-based immunotherapy (3-6). This unmet clinical need has prompted us to develop a novel strategy for the treatment of multiple STS histotypes (7).

Adoptive immunotherapy with T lymphocytes redirected by tumor antigen (TA)-specific chimeric antigen receptors (CAR) is one of the most effective therapy in B-cell malignancies (8-10). However, application of CAR.T cells to solid tumors remains challenging (11-15). Here, we have tested the ability of cytokine-induced-killer T-lymphocytes (CIK) engineered with a TA-specific CAR to target tumor cells obtained by multiple STS hystotypes *in vitro* and *in vivo.* CIK are patient-derived polyclonal T-NK lymphocytes endowed with HLA class I-independent antitumor activity, mediated mostly by the interaction of their NKG2D receptor with stress-inducible targets (MIC A/B; ULBPs 1-6) on tumor cells (16-26). To increase their tumor cell specificity, CIK were engineered with a TA-specific CAR. CAR engineered CIK have been modeled in hematological malignancies to target either CD19 or CD33/CD23 antigens (27-31), and clinical trials are currently ongoing. We and others studied the use of CAR expressing CIK in STS (32-35). In our previous study, we demonstrated the preclinical effectiveness of CAR-redirected CIK against CD44v6, which is expressed in about 40% of STS (32). Here we assessed whether alternative TA could be targeted via CAR engineered immune cells in STS to further expand their clinical applicability.

The TA chondroitin sulfate proteoglycan 4 (CSPG4), a cell surface proteoglycan that plays an important role in oncogenic pathways involved in cancer progression and metastatic spread (36-42), was selected as the target for the following reasons. CSPG4 is highly expressed with limited heterogeneity on both differentiated cancer cells and cancer initiating cells (CICs) in several types of cancer. According to the cancer stem cell hypothesis, CICs play a major role in disease recurrence and metastatic spread, the two major causes of patients' mortality and morbidity. In contrast, CSPG4 is not detectable in normal tissues. Furthermore, CSPG4 is expressed by activated pericytes in the tumor microenvironment (43). As a result, CSPG4 immuno-targeting selectively inhibits neoangiogenesis in the tumor microenvironment, thus contributing to the elimination of the vasculature that supports tumor growth (44).

This manuscript describes the *in vitro* and in vivo ability of CSPG4-CAR.CIK to eliminate STS cells following a description of CSPG4 expression on multiple STS cells.

Materials and Methods

Data analysis of CSPG4 RNA expression in The Cancer Genome Atlas

RNA-sequencing expression data were selected and downloaded from the cBioPortal, TCGA PanCancer collections (45,46). The dataset included 251 STS samples: Leiomyosarcoma n=99, Dedifferentiated Liposarcoma n=58, UPS/Malignant Fibrous Histiocytoma/High-Grade Spindle Cell Sarcoma n=50, Myxofibrosarcoma n=25, Malignant Peripheral Nerve Sheath Tumor (MPNST) n=9, and Synovial Sarcoma n=10. Another 336 melanomas served as a positive expression control and various epithelial tumors (Breast Cancer n=1082, Pancreatic Cancer n=176, Lung Adenocarcinoma n=510, Lung Squamous Cell Carcinoma n=482) were explored for comparison. RSEM expression values were plotted after Log_2 transformation with 0.5 jittering on the x-axis using Microsoft Excel®.

Soft Tissue Sarcoma (STS) cell lines and STS spheroids

STS cell lines were generated in our laboratory from patient-derived surgical biopsies (47). We received approval for collection of patient samples and the associated informed consent document from the Institutional Review Board (IRB) per Declaration of Helsinki guidelines (Prot. Number 225/2015); each patient signed an informed consent. Patient-derived STS were cultured in either KO DMEM F12 (KO Out Dulbecco's Modified Eagle Medium, Gibco BRL) or IMDM (Iscove's Modified Dulbecco Medium, Sigma Aldrich) medium, with 10% or 15% FBS, 25 mmol/L HEPES, 100 U/mL penicillin, and 100 U/mL streptomycin (Gibco BRL) in a humidified 5% CO_2 incubator at 37°C. Patient-derived melanoma cell line M14 (48), which does not express CSPG4, was used as a specificity control and cultured in RPMI 1640 medium (Sigma Aldrich), supplemented with 10% heat inactivated FBS, 100 U/mL penicillin, and 100 U/ mL streptomycin (Gibco BRL) at 37°C in a 5% CO_2 incubator. The HT1080 cell line used in this study was originally obtained from the American Type Culture Collection (ATCC), and was authenticated by genotype analysis with the Cell ID system (Promega) that compared their profile with those published on the DMSZ database. Adult and neonatal keratinocytes were cultured with the Lonza KGM™ Gold Keratinocyte Growth Medium Bullet Kit™.

Three-dimensional STS spheroids were generated as a single spheroid per well using ultra-low attachment (ULA) 96-well round bottom plates (Corning) with no additional coating. A STS cell suspension of between 500 and 5000 cells/100 µl was plated into wells and then centrifuged at 1000 g for 10 min (33). STS spheroids were assembled in 1-4 days, depending on the target histotypes. We generated GFP^+ STS spheroids from cells previously transduced with the pRRL.sin.PPT.hOct4.eGFP.Wpre VSV-G pseudo-typed third-generation lentiviral vector.

Generation of CSPG4-CAR.CIK

Supernatants containing retroviral particles encoding CAR specific for the CSPG4 antigen (CSPG4-CAR) or the control vector encoding CAR specific for the CD19 antigen (CD19-CAR), both containing 4-1BB costimulatory endodomains were generated as previously described (41). We generated CSPG4-CAR.CIK and CSPG4-CAR.T cells from peripheral blood mononuclear cells (PBMC) isolated from patients diagnosed with STS by density gradient centrifugation using Lymphosep (Aurogene). Approval was obtained from the IRB per the Declaration of Helsinki guidelines for the collection of biological samples (tumors and blood) and for patient informed consent releases (Prot. Number 225/2015). For CAR.CIK, PBMC from 8 patients with STS (Suppl. Table 1) were seeded on day 0 in cell culture flasks at a concentration of 2 x 10^6 cells/mL with IFNγ (Miltenyi Biotec; 1000 U/mL) in RPMI-1640 medium (Gibco BRL), 10% FBS (Sigma), 100 U/mL penicillin, and 100 U/mL streptomycin (Gibco BRL). Following a 24 hour incubation at 37°C, PBMC were activated by Anti-Biotin MACSiBead Particles loaded with anti-CD2, -CD3, and -CD28 mAbs (Miltenyi Biotec) and human interleukin (IL)-2 IS (Miltenyi Biotec, 300 U/mL). To generate CAR.T cells, PBMC were seeded on day 0 at a concentration of 2 x 10^6 cells/mL and activated using Anti-Biotin MACSiBead Particles. On day +1, human interleukin (IL)-2 IS (Miltenyi Biotec, 50 U/mL) was added. On day +2, PBMC were transduced with 0.5 ml of retroviral supernatants in retroNectin™-coated plates by overnight incubation. Unmodified NTD.CIK and NTD.T cells were used as a paired control. Both CAR.CIK and control NTD.CIK were expanded over 4 weeks, refreshed with IL-2 medium (CIK: 300 U/mL) every 2–3 days as needed, and cultured at 1.8 x 10^6 cells/mL. CAR.T cells were cultured at 1.8 x 10^6 cells/mL for 1 week, and the IL-2 (50 U/mL) medium was refreshed every 2–3 days as needed.

Flow cytometry

Conjugated CD3, CD4, CD8, CD56, PD-1, CXCR3, CXCR4, and CCR7 mAbs (BD Pharmingen) and CD45RO, CD45RA, and CD62L mAbs (Miltenyi Biotec) were used to characterize lymphocytes. A mAb specific for the IgG1/CH2CH3 spacer (Jackson ImmunoResearch) was used to detect CAR expression. STS cells were stained with conjugated mAbs for the expression of CIK NKG2D ligands MIC A/B (BD Pharmingen) and ULBPs (R&D Systems), and for the expression of HLA-ABC, PD-L1 and PD-L2 (BD Pharmingen). STS were stained for CSPG4 with mAbs 225.28, 763.74, and D2.8.5-C4B8 (49), which recognize distinct and spatially-distant epitopes of CSPG4. Cells were incubated first with CSPG4-specific mAbs (1 µg/mL for all mAbs), then washed and incubated with rabbit anti-mouse IgG-PE secondary antibody (Miltenyi Biotec). Alternatively, CSPG4 was detected with the conjugated anti-human CSPG4-APC mAb (Miltenyi Biotec). CSPG4 molecules expressed on the surface of STS and other cell lines were measured using a quantitative immunofluorescence assay (Bangs Laboratories, Inc.). Briefly, cells of interest and calibration beads with increasing amounts of antibody capture

capability were labeled simultaneously with the anti-human CSPG4-APC mAb. Labeled cells and calibration beads were analysed, and a standard regression line was calculated between fluorescence intensity and antigen density, expressed as Ab-binding capacity (ABC) in molecules per cell. We defined high CSPG4 expression as 2-fold increase as compared to normal keratinocytes. Labeled cells were acquired on FACS Cyan (Cyan ADP, Beckman Coulter s.r.l.) and analyzed using Summit Software.

Tumor cell killing assays

We assessed the tumor-killing ability of patient-derived CSPG4-CAR.CIK and unmodified NTD.CIK *in vitro* against STS cell monolayers and STS 3D spheroids. In two cases, CIK and STS cell cultures were generated from samples collected from the same patient (S1 and S172), while in all other cases cytotoxicity assays were performed with HLA mismatched effector cells. Cytotoxicity assays against STS cell monolayers were performed using flow cytometry or a bioluminescent cell viability assay. In the first case, target cells were stained with either vital dye PKH26 (Sigma-Aldrich) or CFSE (5,6-carboxyfluorescein diacetate succinimidyl ester; Molecular Probes), according to the manufacturer's protocols. Immune-mediated killing was analyzed by flow cytometry (Cyan ADP, Dako) and measured by the DAPI permeability of target cells ($PKH26^+$ or $CFSE^+$ gate). For the bioluminescent method, cytotoxicity was measured with the CellTiter-Glo®Luminescent Cell Viability Assay (Promega), in which the number of viable and metabolically active target cells is evaluated by quantifying the ATP in culture. CIK cells were co-cultured at different effector to target cell ratios (10:1, 5:1, 2.5:1, 1:1, 1:2, and 1:4) in cytotoxicity assays (300 U/mL IL-2 medium at 37°C and 5% CO_2) for 5 hours (short-term assay) and 48 hours (long-term assay). In selected experiments, we tested the cytotoxic activity at very low effector to target cell ratios (1:8, 1:16, 1:32, and 1:64). Target cells were also tested separately from CIK cells as a control to assess their spontaneous mortality. The percentage of STS specific lysis for each effector to target cell ratio was calculated using the following formula: [(experimental−spontaneous mortality/100−spontaneous mortality) × 100]. In selected experiments, growth of residual sarcoma cells was investigated 48 hours after the treatment with either CSPG4-CAR.CIK or NTD.CIK.

In 3D assays, STS spheroids stably expressing GFP were seeded one per well in ULA 96-well round bottom plates. CSPG4-CAR.CIK and unmodified NTD.CIK were stained with PKH26 dye and plated at E:T ratio 2:1 in culture medium with 300 U/mL IL-2 at 37°C, 5% CO_2. Fluorescence images were acquired at 12 hour intervals over 96 hours under the same magnification (10x). Killing activity was determined as loss of GFP fluorescent spheroid area (pixel) using fluorescent microscopy (Leica DMI 3000B equipped with Photometrics CoolSnap HQ CCD camera). Untreated STS spheroids were used to evaluate spontaneous mortality. All images were analysed with ImageJ software, and percentage of tumor cell lysis was determined by the formula: [100 - (treated GFP^+ STS spheroid (pixel) x 100 / untreated GFP^+ STS spheroid (pixel)].

Immunofluorescence analysis of CSPG4-CAR.CIK cell recruitment and infiltration in STS spheroids

GFP^+ STS spheroids were co-cultured with CSPG4-CAR.CIK or unmodified NTD.CIK cells stained with red dye PKH26 at E:T ratio 2:1 in culture medium (300 U/mL IL-2 at 37°C, 5% CO_2). Following a 16 hour co-culture at 37°C, CIK cells were removed and immunofluorescence acquisition was conducted on the remaining spheroids. Briefly, STS spheroids were washed twice, and then centrifuged at 300 g for 3 min in PBS, fixed in paraformaldehyde 4% for 1 hour, resuspended with mounting medium, and applied on either glass slides or glass bottom chamber slide wells. STS spheroids were observed using a Leica SP8 AOBS confocal microscope. Next, 80MHz pulsed white light laser (470-670 nm) was used to excite the fluorochromes in the spheroids. Fluorescence channels were scanned sequentially, and hybrid spectral detectors (HyD SP Leica Microsystems) revealed the emissions. Image acquisition of the STS spheroids was performed maintaining the same laser power, gain, offset, and magnification (20x). We generated maximum intensity projections for each analysed spheroid with LAS X software (Leica) to quantify CIK cell recruitment and infiltration. Images of the total PKH26 red fluorescent area (μm^2) present either at the boundary or inside the spheroid were analysed using ImageJ software.

CIK cell penetration capability into Matrigel® matrix

STS spheroids were collected, washed in PBS, resuspended in 20 µl of liquefied Matrigel® (BD Pharmingen) at 4°C, and then plated as droplets in well centres of a 24-well tissue culture plate that had been pre-warmed to 37°C. Plates were incubated at 37°C and 5% CO_2 for 15 min to allow the solidification of the Matrigel® domes. Domes were then overlaid with 500 µl of pre-warmed medium with 300 U/mL IL-2 and co-cultured with PKH2-stained CSPG4-CAR.CIK or unmodified NTD.CIK cells (50.000 cells/well) for 5 days. Empty domes were used as controls. At the end of the co-culture period, each well was washed twice with pre-warmed PBS to eliminate any effector cells outside the domes. Fluorescence microscopy (Leica DMI 3000B with Photometrics CoolSnap HQ equipped with CCD camera) was used to visualise CSPG4-CAR.CIK or unmodified NTD.CIK cell migration at the Matrigel® boundary and cells that penetrated into the Matrigel® domes. Analysis of the PKH26 red fluorescent dye presence (μm^2) was performed with ImageJ software.

***In vitro* cytokine production**

CSPG4-CAR.CIK and CSPG4-CAR.T cells, unmanipulated NTD.CIK and NTD.T cells were co-cultured alone or with tumor cells in RPMI 1640 medium with 300U/ml (CIK) or 50U/ml IL-2 (T cells) at a 2:1 effector-to-target ratio and incubated at 37°C for 48 hours. Concentrations of cytokines in culture supernatant were measured using the Bio-Plex Pro™ Human Cytokine 9-plex Assay kit (Bio-Rad Laboratories Inc.) according to the manufacturer's directions. Each sample was measured in duplicate. Data were acquired and analysed by

Bioclarma (Analysis Service). Granzyme B concentration was measured in supernatants from mixed target/effector cell cultures (ELISA Granzyme B kit; Diaclone SAS, Besancon, France), as recommended by the manufacturer.

In vivo activity of patient-derived CSPG4-CAR.CIK

The antitumor activity of CSPG4-CAR.CIK and unmodified NTD.CIK was evaluated using STS xenograft models in immunodeficient mice. *In vivo* experiments received approval by the competent committee and internal review board (Auth. Number 178/2015-PR). STS xenografts were established in seven- to eight-week-old NOG/SCID/$\gamma c^{-/-}$ (NSG) or NOD/SCID (Charles River Laboratories, SRL, Italy) female mice by subcutaneous injection with $1x10^6$ cells obtained from three STS [fibrosarcoma (HT1080), leiomyosarcoma (S172), UPS (S1)]. Autologous CSPG4-CAR.CIK and unmodified NTD.CIK were available for S172 and S1 xenografts. Allogeneic CSPG4-CAR.CIK from unrelated STS patients were generated following the same protocol used to generate autologous CIK identical and used in the HT1080 xenograft model. When tumors were approximatively 50 mm^3, mice were infused twice a week with $1x10^6$ CSPG4-CAR.CIK or unmodified NTD.CIK resuspended in PBS (200 µL), for a total of four infusions. Mice injected with PBS only were used as controls. Treatment and control cohorts included 6 mice each for the leiomyosarcoma (S172) group. For the fibrosarcoma (HT1080) and UPS (S1) xenografts and control groups, each group included 3 mice. In the experiments with fibrosarcoma (HT1080) and leiomyosarcoma (S172), mice were sacrificed at the end of treatment. In the experiment with UPS (S1), mice were sacrificed 14 days after the last CIK infusion. Mice were monitored daily for possible toxicities, while tumor growth was measured weekly with manual caliper. Mice were sacrificed at the end of treatment or if tumor reached 2 cm along the main diameter. In additional experiments mice engrafted with the S172 cell line (n = 4 mice per treatment) or the HT1080 cell line (n = 5 mice per treatment) were infused with CSPG4-CAR.CIK and unmodified NTD.CIK generated from unrelated donors. In these models, when the tumor volume was approximatively 20 mm^3, mice received two infusions (on day 0 and day +4) of $3x10^6$ CSPG4-CAR.CIK or unmodified NTD.CIK. Mice were sacrificed 11 days after the last dose of cells. Tumor volume was calculated by the following formula: $V= 4/3 \times \pi \times (a/2)^2 \times (b/2)$, where a is the length and b is the width of the tumor.

Immunohistochemistry (IHC)

STS xenografts were analysed by IHC to assess CSPG4 expression. Samples (5-µm thick) were cut from formalin-fixed paraffin-embedded (FFPE) tissue sections, mounted on slides, and treated as per standard immunohistochemistry procedures. Tissue sections were deparaffinised with 100% xylene and rehydrated with decreasing concentrations of ethyl alcohol. Antigen retrieval was performed by boiling the sections in 1 mM EDTA (pH 9.0) for 60 min. Slides were treated with 3% hydrogen peroxide, 1% bovine serum albumin (BSA) (Invitrogen), and 5% normal horse serum in Tris-buffered saline (25 mM Tris [pH 7.4], 150 mM NaCl) containing 0.1% Tween 20 (Sigma-Aldrich, Inc). Slides were then incubated in a closed humid chamber overnight at 4°C with the CSPG4-specific mAb 225.28, 763.74, and D2.8.5-C4B8 (4 µg/ml each) pool. After washing, a secondary anti-mouse IgG xenoantibody was added. Secondary antibodies conjugated to HRP were generated and IHC signals were detected with the EnVision1® System-HRP (Dako North America, Inc) and chromogen diaminobenzidine (DAB) substrate (DakoCytomation Liquid DAB+ Substrate Chromogen System, Dako). Tissue sections were counterstained with Mayer Haematoxylin (Bio-Optica). We also explored the presence of infiltrated CSPG4-CAR.CIK, unmodified NTD.CIK cells and apoptotic tumor cells in explanted tumors from treated mice. Tissues were stained according to the manufacturer's protocols with the primary polyclonal antibody anti-CD3 (DAKO) and anti-cleaved caspase 3 (Cell Signalling). Tissue sections were mounted on glass slides and visualized with a DM750 Leica microscope equipped with Leica ICC50W CCD camera (LAS EZ3.4.0 software).

Statistical analysis

All experiments were performed at least twice. Data were analyzed using GraphPad Prism 8.0 (GraphPad Software, La Jolla, CA). Descriptive data are presented as mean values ± standard errors. To find statistical significance in the comparison of two groups, we used two-tailed Student's t-tests; for comparison of three or more groups, the data were analyzed by two-way ANOVA with Bonferroni's multiple comparison post-tests. A p-value < 0.05 was considered significant. Significance is represented on graphs as $*P \leq 0.05$, $**P \leq 0.01$, $***P \leq 0.001$, and $****P \leq 0.0001$.

Results

Generation and characterization of patient-derived CSPG4-CAR.CIK.

CIK cells were efficiently generated from peripheral blood mononuclear cells (PBMCs) collected from eight patients diagnosed with STS. We genetically engineered CIK to express the CSPG4-CAR that includes the 4-1BB costimulatory endodomain. Three weeks following transduction and *ex vivo* expansion, the mean expression of CAR on engineered CIK (CSPG4-CAR.CIK) was 48% ±6 as assessed by flow cytometry (Suppl. Table 1 and in Suppl. Fig 1A) and was comparable to that obtained using the retroviral vector encoding the CD19-specific CAR (CD19-CAR). *Ex vivo* expansion of CSPG4-CAR.CIK was 154-fold (27-348) and was comparable to that observed with paired control unmodified CIK (NTD.CIK). The phenotypic characterization of CSPG4-CAR.CIK was comparable to that of paired unmodified NTD.CIK showing $CD8^+$ cells as the main cellular subset (69% ±4) of which 39% ±5 of them co-expressed the CD56 molecule ($CD3^+CD56^+$) (Suppl. Table 1). The NKG2D receptor was 66% ±5, and 47% ±0.1 of the cells were $CD62L^+CD45RA^-$, the latter represent the effector-memory-like population (Suppl. Fig. 1B). The immune-checkpoint receptor PD-1 was expressed on 12% ±2 in both CSPG4-CAR.CIK and NTD.CIK (Suppl. Table 1).

CSPG4 as a potential CAR target in STS.

We confirmed first that CSPG4 is expressed in multiple STS histotype cells (Leiomyosarcoma; Dedifferentiated Liposarcoma; Undifferentiated pleomorphic sarcoma (UPS), Malignant Fibrous Histiocytoma, High-Grade Spindle Cell Sarcoma; Myxofibrosarcoma; Malignant Peripheral Nerve Sheath Tumor (MPNST); Synovial Sarcoma) at levels similar to those found in melanoma cells (Fig1 A) by *in silico* with RNA-sequencing expression data from the TCGA database. Furthermore, using flow cytometry we observed CSPG4 expression on the cell surface of 15 out of 15 STS cell lines obtained from biopsies of patients affected by different histotypes of advanced STS (UPS n=3, GIST n=5, Liposarcoma n=4, Leiomyosarcoma n=2, MPNST n=1) and in the HT1080 cell line (Fibrosarcoma) from ATCC (Fig 1B).

CSPG4 density on STS cell lines was quantified on per cell basis and found variable among STS samples (mean of 321±47 molecules per cell) (Fig. 1C). STS cell lines were also confirmed to express variable levels of the main known ligands recognized by the NKG2D CIK receptor (MIC A/B: 30% ±8; ULBP1: 1 %±0.7; ULBP2/5/6: 71%±6; ULBP3: 25%±9). HLA class-I antigens are highly expressed by all STS cell lines tested (95%±2), along with varying levels of immune-checkpoints PD-L1 (32%±9) and PD-L2 (65%±6) (Suppl. Table 2).

CSPG4-CAR.CIK effectively and specifically target STS *in vitro*.

We explored the *in vitro* anti-tumor activity of CSPG4-CAR.CIK against 12 STS cell lines. In 2 cases (S1 UPS and S172 Leiomyosarcoma) it was possible to obtain peripheral blood from the patient from whom the STS tumor cell line was generated. At effector-to-target cell ratios (E:T) from 10:1 to 1:4, CSPG4-CAR.CIK revealed significantly superior *in vitro* cytotoxicity against STS (Figure 2A and Suppl. Figure 2A), as compared to that

reported with unmodified NTD.CIK (n=29; p<0.0001). Furthermore, the anti-tumor activity of CSPG4-CAR.CIK was maintained even at very low E:T ratios (1:8 to 1:64) (n=8; p<0.0001, Figure 2B).

CSPG4-CAR.CIK antitumor activity was superior to that of control CD19-CAR.CIK (n=5, p<0.05, Figure 2C) and was CSPG4-specific because CSPG4-CAR.CIK did not eliminate non-expressing CSPG4 target cells (n=3, p>0.05, Figure 2D). Finally, at E:T ratios that mediate potent antitumor effects, CSPG4-CAR.CIK had no detectable activity against human keratinocytes that show low CSPG4 expression (n=5, Figure 2E). CSPG4-CAR.CIK-mediated tumor elimination was strictly dependent on the CSPG4 expression level on tumor cells (n=7, p<0.05, Figure 2F).

We also measured the antitumor activity of CSPG4-CAR.CIK cells in a STS sample expressing CSPG4, but lacking NKG2D ligands, and found that CAR expression per se promotes antitumor activity of redirected CIK independently from NKG2D CIK receptor engagement (p<0.001, Figure 2G).

Following treatment with CSPG4-CAR.CIK, we evaluated if residual tumor cells spared by the cytotoxic effects of CIK may regrow. We observed significant delayed *in vitro* re-growth of STS cells exposed to CSPG4-CAR.CIK (48 hours after treatment) as compared with tumor cells exposed to unmodified NTD.CIK (n=2, p<0.05, Figure 2H).

A significant and superior (three-fold E:T 5:1) activity level of STS killing was displayed by CSPG4-CAR.CIK compared to CAR.T lymphocytes. Both effector cells were generated from PBMC collected from the same patient and expressed comparable levels of CSPG4-specific CAR molecules (n=2, p<0.001, Figure 2I, Suppl. Figure 3A,B).

In selected experiments, we explored the production of Th1- and Th2-type cytokines and granzyme B by CSPG4-CAR.CIK at baseline and following exposure to STS CSPG4-positive targets. Overall, we observed higher baseline productions of IFNγ, IL-6, IL1β, IL-4, IL-8, GM-CSF, TNFα, IL-10, and granzyme B by CSPG4-CAR.CIK that markedly increased following engagement with STS CSPG4-positive targets (n=4) (Suppl. Figure 4A). The highest cytokine peaks were observed for IFNγ, IL-6, IL-8, TNFα, and GM-CSF. The most differentially expressed cytokines by CSPG4-CAR.CIK in response to CSPG4 expressing STS as compared to NTD.CIK were: IFNγ (80-fold), IL1β (4.5-fold), IL-6 (1.3-fold), TNFα (7.6-fold), GM-CSF (88.5-fold), IL-10 (16-fold), IL-8 (1.3-fold), IL-4 (7-fold) and granzyme B (20-fold). Complete cytokine values, including CAR.T lymphocytes control, are reported in Supplemental Figure 4B.

CSPG4-CAR.CIK effectively target STS cells in 3D spheroids.

We developed the STS spheroid model that mimics tumor three-dimensionality (3D) and allows exploring CAR.CIK migration in a multidimensional structure. STS spheroids express GFP, which allows tracking their fate by longitudinal imaging. Spheroids were generated for three STS (S1, S5 and S172). Spheroids were co-incubated with effector cells at E:T ratio 2:1, and loss of fluorescence over time was considered as a surrogate indication of tumor elimination by CSPG4-CAR.CIK (Figure 3A,B). CSPG4-CAR.CIK eliminated STS spheroids more effectively than unmodified NTD.CIK (n=3, $p<0.0001$) (Figure 4A-C).

In selected experiments, we also used live imaging to visualize the antitumor kinetics of CSPG4-CAR.CIK against STS spheroids (Supplemental Video 1, 2). Furthermore, measurement of the maximum intensity projections of S172 and S5 spheroids after incubation with CSPG4-CAR.CIK or unmodified NTD.CIK indicated that CSPG4-CAR.CIK were present at a higher concentration within the STS spheroids as compared to unmodified NTD.CIK (n=8, $p<0.05$, Figure 4D-F) (Supplemental Video 3-6). Finally, in selected experiments, we measured the capability of CSPG4-CAR.CIK to penetrate and migrate toward STS spheroids through Matrigel® domes, with the intent of mimicking their dynamics through the extracellular matrix (Figure 5A). Microscopic inspection indicated that CSPG4-CAR.CIK readily migrated to the membrane boundary and penetrated the Matrigel® domes containing STS spheroids more efficiently than unmodified NTD.CIK cells (n=5, $p<0.01$, Figure 5B, C).

CSPG4-CAR.CIK controlled tumor growth *in vivo*.

We explored the *in vivo* antitumor activity of CSPG4-CAR.CIK utilizing three STS xenograft models (HT1080 Fibrosarcoma, S172 Leiomyosarcoma, and S1 UPS) that were selected because of the different levels of CSPG4 expression. Upon tumor engraftment (~50 mm^3) mice were treated with intravenous infusions of CSPG4-CAR.CIK or unmodified NTD.CIK (Figure 6A). In two models (S1 and S172) CIK and tumor cells were autologous, while CAR.CIK tested in the HT1080 xenograft model were allogeneic. In the S172 leiomyosarcoma xenograft model characterized by 72% CSPG4 expression and a density of 262 molecules/cell, autologous CSPG4-CAR.CIK, but not unmodified NTD.CIK or vehicle, caused significant delay in tumor growth ($p<0.05$) (n=6 mice/group) (Figure 6B). In the HT1080 fibrosarcoma and S1 UPS xenograft models showing 23% and 95% CSPG4 expression, respectively, but similar densities of target molecules (521 and 499 mol/cell, respectively), CSPG4-CAR.CIK also delayed tumor growth as compared to controls ($p<0.001$ HT1080; $p<0.0001$ S1) (n=3 mice/group) (Figure 6C, D). Tumor infiltration by CSPG4-CAR.CIK was confirmed in explanted tumors by IHC (Figure 6E). Cleaved caspase 3 levels were confirmed higher in tumors from mice treated with CSPG4-CAR.CIK as compared to those from NTD.CIK treated or vehicle-treated mice (Figure 6F). The antitumor activity of CSPG4-CAR.CIK was also verified in additional experiments in which we reduced the initial tumor burden (~20 mm^3) for both HT1080 and S172 tumors (Suppl. Figure 5A). In these models, CSPG4-CAR.CIK treatment resulted in significant delay of tumor growth up to 11 days after the end of treatment as

compared to controls ($p<0.001$ HT1080; $p<0.0001$ S172) (Suppl. Figure 5B-E). A complete tumor regression was observed in 2 out of 4 mice bearing leiomyosarcoma and 1 out 5 mice bearing fibrosarcoma (HT1080). Of note, antitumor effects were obtained without any macroscopic evidence of toxicity.

Discussion

STS are tumors for which the clinical impact of targeted therapies remains modest (3). Here, we report that CSPG4 is a clinically relevant target in STS and that CSPG4 expression can be efficiently exploited to eliminate STS tumors by redirecting the specificity of CIK through CAR engineering. We generated compelling evidence supporting the antitumor activity of CAPG4-CAR.CIK using cell lines derived from patients who relapsed after conventional treatments and developing an experimental platform that includes *in vitro* bi-dimensional and three-dimensional assays along with three distinct *in vivo* STS xenograft models.

The survival rate of adults and children with STS remains extremely poor even in the era of checkpoint inhibitors (3,50,51). The latter disappointing clinical results are likely to be caused at least in part by the "cold" or "immunologically-ignorant" tumor microenvironment, low neoantigen load and defects in HLA class I antigen-presenting machinery in STS (3,52).

Adoptive transfer of *ex vivo* engineered effector T cells, and in particular CAR.T cells, providing HLA-independent tumor recognition may offer the possibility to elicit immune responses in otherwise silent tumors such as STS. However, the identification of the most appropriate antigen to be recognized by CAR.T cells in STS remains to be defined. Here we show that CSPG4 holds critical biological features to qualify as a valuable target candidate in STS (38,41). Using the TCGA dataset we found that CSPG4 mRNA is highly expressed in STS across multiple histotypes. Furthermore, we confirmed CSPG4 protein expression on the cell surface of a wide array of STS cell lines spanning multiple STS histotypes and derived from patients who relapsed after conventional treatments. This information is critical in the clinical setting because STS are intrinsically highly heterogeneous especially in relapsed patients (1). Importantly, CSPG4 expression in all these tumor cell lines was identified by the antibody that we have used to generate the CSPG4-specific CAR and previously used to show the limited expression of CSPG4 in normal healthy tissues as compared to multiple solid tumors, despite broad CSPG4 mRNA expression in various organs (37,53). In the perspective of a clinical application, a systematic confirmation of CSPG4 expression by IHC in STS sections that include tumor microenvironment would be warranted.

As for the majority of non-lineage restricted markers, the density of CSPG4 expression in STS cell lines was variable, but in general much higher of the expression detected in normal keratinocytes. We found a correlation between CSPG4 expression level and anti-tumor activity by CSPG4-CAR redirected CIK with minimal activity against normal keratinocytes. The latter finding is consistent with previous data underscoring the importance of antigen density to define a therapeutic window for antigens that are expressed, although at low levels, also by normal tissues (54,55).

While CAR-redirected effector T cells showed potent antitumor effects in B cell malignancies, it remains to be defined if other cell subtypes such as NK cells, NKT cells or $\gamma\delta$T cells may possess intrinsic biologic characteristics to be exploited in solid tumors to enhance the therapeutic index of engineered immune cells

(12). Here, rather than exploring different immune cell subsets, we propose that T cells with enhanced cytokine-activation during the *ex vivo* expansion such as CAR-engineered CIK may represent a valid cellular platform for the treatment of STS. Dosing and prolonged *ex vivo* exposure to IL-2 induces a mixed T-NK phenotype and function in CIK lymphocytes with variable degree of HLA-independent (NKG2D mediated) tumor killing ability (56). We reasoned that CAR engineered CIK would exploit dual tumor cell-killing potential namely antigen independent via NKG2D receptor engagement and antigen-dependent via CSPG4-CAR engagement. The utilization of these two mechanisms is expected to ultimately amplify the antitumor effects of CSPG4-CAR.CIK and potentially counteract the escape mechanisms utilized by tumor cells with low CSPG4 expression. We found that CAR.CIK exerted potent antitumor effects against a wide array of STS, which was particularly evident at very low effector to target cell ratios.

The activity of CSPG4-CAR.CIK was confirmed in three independent STS xenograft models and showed clearly gain of function by CIK cells expressing the CAR as compared to unmodified NTD.CIK further supporting the evidence that NKG2D and CAR engagement are not mutually exclusive in CAR engineered CIK. Our study using relatively simple 3D assays to explore the dynamic features of CAR.CIK *ex vivo* in a more complex structure compared to liquid culture also uncovered remarkable migratory and infiltrative abilities of CAR engineered CIK. These properties further underline the potential impact of these cells in solid tumors. It is important to acknowledge that clinical data indicate that CIK are more terminally differentiated as compared to activated and expanded T cells. As a result their longevity *in vivo* upon adoptive transfer may be limited (32,57). However, clinical data also indicate that the manufacturing of CIK both unmanipulated or CAR engineered is very robust. This property allows logarithmic expansion of cells in a relatively short period of time and storing of CIK for multiple infusions. Furthermore the initial evidence of a lower IL-1β and IL-6 production by CAR.CIK as compared to paired “conventional” CAR.T lymphocytes, may further support a favorable safety profile.

Overall, our data support CSPG4 as a valuable CAR-target for STS and the use of CIK engineered to express the CSPG4-specific CAR for the development and implementation of a novel and effective immunotherapeutic strategy for the treatment of patients with advanced/relapsed high-grade STS.

Acknowledgments: The authors sincerely thank Joan Leonard (Leonard Editorial Services, LLC) for the linguistic revision and editorial assistance.

References

1. Siegel RL, Miller KD, Jemal A. Cancer statistics, 2019. CA Cancer J Clin **2019**;69(1):7-34 doi 10.3322/caac.21551.
2. Pasquali S, Pizzamiglio S, Touati N, Litiere S, Marreaud S, Kasper B*, et al.* The impact of chemotherapy on survival of patients with extremity and trunk wall soft tissue sarcoma: revisiting the results of the EORTC-STBSG 62931 randomised trial. Eur J Cancer **2019**;109:51-60 doi 10.1016/j.ejca.2018.12.009.
3. Pollack SM, Ingham M, Spraker MB, Schwartz GK. Emerging Targeted and Immune-Based Therapies in Sarcoma. J Clin Oncol **2018**;36(2):125-35 doi 10.1200/JCO.2017.75.1610.
4. Wisdom AJ, Mowery YM, Riedel RF, Kirsch DG. Rationale and emerging strategies for immune checkpoint blockade in soft tissue sarcoma. Cancer **2018**;124(19):3819-29 doi 10.1002/cncr.31517.
5. Alsaab HO, Sau S, Alzhrani R, Tatiparti K, Bhise K, Kashaw SK*, et al.* PD-1 and PD-L1 Checkpoint Signaling Inhibition for Cancer Immunotherapy: Mechanism, Combinations, and Clinical Outcome. Front Pharmacol **2017**;8:561 doi 10.3389/fphar.2017.00561.
6. Donini C, D'Ambrosio L, Grignani G, Aglietta M, Sangiolo D. Next generation immune-checkpoints for cancer therapy. J Thorac Dis **2018**;10(Suppl 13):S1581-S601 doi 10.21037/jtd.2018.02.79.
7. Pollack SM, Loggers ET, Rodler ET, Yee C, Jones RL. Immune-based therapies for sarcoma. Sarcoma **2011**;2011:438940 doi 10.1155/2011/438940.
8. Jacoby E, Shahani SA, Shah NN. Updates on CAR T-cell therapy in B-cell malignancies. Immunol Rev **2019**;290(1):39-59 doi 10.1111/imr.12774.
9. Grupp SA, Kalos M, Barrett D, Aplenc R, Porter DL, Rheingold SR*, et al.* Chimeric antigen receptor-modified T cells for acute lymphoid leukemia. N Engl J Med **2013**;368(16):1509-18 doi 10.1056/NEJMoa1215134.
10. Vera J, Savoldo B, Vigouroux S, Biagi E, Pule M, Rossig C*, et al.* T lymphocytes redirected against the kappa light chain of human immunoglobulin efficiently kill mature B lymphocyte-derived malignant cells. Blood **2006**;108(12):3890-7 doi 10.1182/blood-2006-04-017061.
11. Gauthier J, Yakoub-Agha I. Chimeric antigen-receptor T-cell therapy for hematological malignancies and solid tumors: Clinical data to date, current limitations and perspectives. Curr Res Transl Med **2017**;65(3):93-102 doi 10.1016/j.retram.2017.08.003.
12. Rotolo R, Leuci V, Donini C, Cykowska A, Gammaitoni L, Medico G*, et al.* CAR-Based Strategies beyond T Lymphocytes: Integrative Opportunities for Cancer Adoptive Immunotherapy. Int J Mol Sci **2019**;20(11) doi 10.3390/ijms20112839.
13. Klebanoff CA, Rosenberg SA, Restifo NP. Prospects for gene-engineered T cell immunotherapy for solid cancers. Nat Med **2016**;22(1):26-36 doi 10.1038/nm.4015.
14. Leuci V, Mesiano G, Gammaitoni L, Aglietta M, Sangiolo D. Genetically redirected T lymphocytes for adoptive immunotherapy of solid tumors. Curr Gene Ther **2014**;14(1):52-62.
15. Newick K, O'Brien S, Moon E, Albelda SM. CAR T Cell Therapy for Solid Tumors. Annu Rev Med **2017**;68:139-52 doi 10.1146/annurev-med-062315-120245.
16. Schmidt-Wolf IG, Lefterova P, Mehta BA, Fernandez LP, Huhn D, Blume KG*, et al.* Phenotypic characterization and identification of effector cells involved in tumor cell recognition of cytokine-induced killer cells. Exp Hematol **1993**;21(13):1673-9.
17. Giraudo L, Gammaitoni L, Cangemi M, Rotolo R, Aglietta M, Sangiolo D. Cytokine-induced killer cells as immunotherapy for solid tumors: current evidences and perspectives. Immunotherapy **2015** doi 10.2217/imt.15.61.
18. Gammaitoni L, Giraudo L, Macagno M, Leuci V, Mesiano G, Rotolo R*, et al.* Cytokine-Induced Killer Cells Kill Chemo-surviving Melanoma Cancer Stem Cells. Clin Cancer Res **2017**;23(9):2277-88 doi 10.1158/1078-0432.CCR-16-1524.

19. Mesiano G, Grignani G, Fiorino E, Leuci V, Rotolo R, D'Ambrosio L*, et al.* Cytokine Induced Killer cells are effective against sarcoma cancer stem cells spared by chemotherapy and target therapy. Oncoimmunology **2018**;7(11):e1465161 doi 10.1080/2162402X.2018.1465161.
20. Kuci S, Rettinger E, Voss B, Weber G, Stais M, Kreyenberg H*, et al.* Efficient lysis of rhabdomyosarcoma cells by cytokine-induced killer cells: implications for adoptive immunotherapy after allogeneic stem cell transplantation. Haematologica **2010**;95(9):1579-86 doi haematol.2009.019885 [pii]10.3324/haematol.2009.019885.
21. Rettinger E, Meyer V, Kreyenberg H, Volk A, Kuçi S, Willasch A*, et al.* Cytotoxic Capacity of IL-15-Stimulated Cytokine-Induced Killer Cells Against Human Acute Myeloid Leukemia and Rhabdomyosarcoma in Humanized Preclinical Mouse Models. Front Oncol **2012**;2:32 doi 10.3389/fonc.2012.00032.
22. Introna M, Golay J, Rambaldi A. Cytokine Induced Killer (CIK) cells for the treatment of haematological neoplasms. Immunol Lett **2013**;155(1-2):27-30 doi 10.1016/j.imlet.2013.09.017.
23. Cappuzzello E, Sommaggio R, Zanovello P, Rosato A. Cytokines for the induction of antitumor effectors: The paradigm of Cytokine-Induced Killer (CIK) cells. Cytokine Growth Factor Rev **2017**;36:99-105 doi 10.1016/j.cytogfr.2017.06.003.
24. Cappuzzello E, Tosi A, Zanovello P, Sommaggio R, Rosato A. Retargeting cytokine-induced killer cell activity by CD16 engagement with clinical-grade antibodies. Oncoimmunology **2016**;5(8):e1199311 doi 10.1080/2162402X.2016.1199311.
25. Li M, Wang Y, Wei F, An X, Zhang N, Cao S*, et al.* Efficiency of Cytokine-Induced Killer Cells in Combination with Chemotherapy for Triple-Negative Breast Cancer. J Breast Cancer **2018**;21(2):150-7 doi 10.4048/jbc.2018.21.2.150.
26. Schmeel LC, Schmeel FC, Coch C, Schmidt-Wolf IG. Cytokine-induced killer (CIK) cells in cancer immunotherapy: report of the international registry on CIK cells (IRCC). J Cancer Res Clin Oncol **2015**;141(5):839-49 doi 10.1007/s00432-014-1864-3.
27. Magnani CF, Mezzanotte C, Cappuzzello C, Bardini M, Tettamanti S, Fazio G*, et al.* Preclinical Efficacy and Safety of CD19CAR Cytokine-Induced Killer Cells Transfected with Sleeping Beauty Transposon for the Treatment of Acute Lymphoblastic Leukemia. Hum Gene Ther **2018**;29(5):602-13 doi 10.1089/hum.2017.207.
28. Marin V, Kakuda H, Dander E, Imai C, Campana D, Biondi A*, et al.* Enhancement of the anti-leukemic activity of cytokine induced killer cells with an anti-CD19 chimeric receptor delivering a 4-1BB-zeta activating signal. Exp Hematol **2007**;35(9):1388-97 doi S0301-472X(07)00348-7 [pii]10.1016/j.exphem.2007.05.018.
29. Marin V, Pizzitola I, Agostoni V, Attianese GM, Finney H, Lawson A, *et al.* Cytokine-induced killer cells for cell therapy of acute myeloid leukemia: improvement of their immune activity by expression of CD33-specific chimeric receptors. Haematologica 2**010;**95(12):2144-52 doi 10.3324/haematol.2010.026310.
30. Pizzitola I, Anjos-Afonso F, Rouault-Pierre K, Lassailly F, Tettamanti S, Spinelli O, *et al.* Chimeric antigen receptors against CD33/CD123 antigens efficiently target primary acute myeloid leukemia cells in vivo. Leukemia 2**014;**28(8):1596-605 doi 10.1038/leu.2014.62.
31. Tettamanti S, Marin V, Pizzitola I, Magnani CF, Giordano Attianese GM, Cribioli E, *et al.* Targeting of acute myeloid leukaemia by cytokine-induced killer cells redirected with a novel CD123-specific chimeric antigen receptor. Br J Haematol 2**013;**161(3):389-401 doi 10.1111/bjh.12282.
32. Leuci V, Casucci GM, Grignani G, Rotolo R, Rossotti U, Vigna E, *et al.* CD44v6 as innovative sarcoma target for CAR-redirected CIK cells. Oncoimmunology 2**018;**7(5):e1423167 doi 10.1080/2162402X.2017.1423167.
33. Merker M, Pfirrmann V, Oelsner S, Fulda S, Klingebiel T, Wels WS, *et al.* Generation and characterization of ErbB2-CAR-engineered cytokine-induced killer cells for the treatment of high-risk soft tissue sarcoma in children. Oncotarget 2**017;**8(39):66137-53 doi 10.18632/oncotarget.19821.
34. Zuo S, Wen Y, Panha H, Dai G, Wang L, Ren X, *et al.* Modification of cytokine-induced killer cells with folate receptor alpha (FRα)-specific chimeric antigen receptors enhances their antitumor

immunity toward FRα-positive ovarian cancers. Mol Immunol 2**017;**85:293-304 doi 10.1016/j.molimm.2017.03.017.

35. Ren X, Ma W, Lu H, Yuan L, An L, Wang X, *et al.* Modification of cytokine-induced killer cells with chimeric antigen receptors (CARs) enhances antitumor immunity to epidermal growth factor receptor (EGFR)-positive malignancies. Cancer Immunol Immunother 2**015;**64(12):1517-29 doi 10.1007/s00262-015-1757-6.
36. Wang X, Wang Y, Yu L, Sakakura K, Visus C, Schwab JH, *et al.* CSPG4 in cancer: multiple roles. Curr Mol Med 2**010;**10(4):419-29.
37. Wang Y, Geldres C, Ferrone S, Dotti G. Chondroitin sulfate proteoglycan 4 as a target for chimeric antigen receptor-based T-cell immunotherapy of solid tumors. Expert Opin Ther Targets 2**015;**19(10):1339-50 doi 10.1517/14728222.2015.1068759.
38. Ilieva KM, Cheung A, Mele S, Chiaruttini G, Crescioli S, Griffin M, *et al.* Chondroitin Sulfate Proteoglycan 4 and Its Potential As an Antibody Immunotherapy Target across Different Tumor Types. Front Immunol 2**017;**8:1911 doi 10.3389/fimmu.2017.01911.
39. Geldres C, Savoldo B, Hoyos V, Caruana I, Zhang M, Yvon E, *et al.* T lymphocytes redirected against the chondroitin sulfate proteoglycan-4 control the growth of multiple solid tumors both in vitro and in vivo. Clin Cancer Res 2**014;**20(4):962-71 doi 10.1158/1078-0432.CCR-13-2218.
40. Harrer DC, Dörrie J, Schaft N. CSPG4 as Target for CAR-T-Cell Therapy of Various Tumor Entities-Merits and Challenges. Int J Mol Sci 2**019;**20(23) doi 10.3390/ijms20235942.
41. Pellegatta S, Savoldo B, Di Ianni N, Corbetta C, Chen Y, Patané M, *et al.* Constitutive and TNFα-inducible expression of chondroitin sulfate proteoglycan 4 in glioblastoma and neurospheres: Implications for CAR-T cell therapy. Sci Transl Med 2**018;**10(430) doi 10.1126/scitranslmed.aao2731.
42. Chekenya M, Krakstad C, Svendsen A, Netland IA, Staalesen V, Tysnes BB, *et al.* The progenitor cell marker NG2/MPG promotes chemoresistance by activation of integrin-dependent PI3K/Akt signaling. Oncogene 2**008;**27(39):5182-94 doi 10.1038/onc.2008.157.
43. Ozerdem U, Stallcup WB. Pathological angiogenesis is reduced by targeting pericytes via the NG2 proteoglycan. Angiogenesis 2**004;**7(3):269-76 doi 10.1007/s10456-004-4182-6.
44. Wang J, Svendsen A, Kmiecik J, Immervoll H, Skaftnesmo KO, Planagumà J, *et al.* Targeting the NG2/CSPG4 proteoglycan retards tumour growth and angiogenesis in preclinical models of GBM and melanoma. PLoS One 2**011;**6(7):e23062 doi 10.1371/journal.pone.0023062.
45. Gao J, Aksoy BA, Dogrusoz U, Dresdner G, Gross B, Sumer SO, *et al.* Integrative analysis of complex cancer genomics and clinical profiles using the cBioPortal. Sci Signal 2**013;**6(269):pl1 doi 10.1126/scisignal.2004088.
46. Cerami E, Gao J, Dogrusoz U, Gross BE, Sumer SO, Aksoy BA, *et al.* The cBio cancer genomics portal: an open platform for exploring multidimensional cancer genomics data. Cancer Discov 2**012;**2(5):401-4 doi 10.1158/2159-8290.CD-12-0095.
47. Sangiolo D, Mesiano G, Gammaitoni L, Leuci V, Todorovic M, Giraudo L, *et al.* Cytokine-induced killer cells eradicate bone and soft-tissue sarcomas. Cancer Res 2**014;**74(1):119-29 doi 10.1158/0008-5472.CAN-13-1559.
48. Luo W, Hsu JC, Tsao CY, Ko E, Wang X, Ferrone S. Differential immunogenicity of two peptides isolated by high molecular weight-melanoma-associated antigen-specific monoclonal antibodies with different affinities. J Immunol 2**005;**174(11):7104-10 doi 10.4049/jimmunol.174.11.7104.
49. Wang Y, Sabbatino F, Wang X, Ferrone S. Detection of chondroitin sulfate proteoglycan 4 (CSPG4) in melanoma. Methods Mol Biol 2**014;**1102:523-35 doi 10.1007/978-1-62703-727-3_28.
50. D'Angelo SP, Mahoney MR, Van Tine BA, Atkins J, Milhem MM, Jahagirdar BN, *et al.* Nivolumab with or without ipilimumab treatment for metastatic sarcoma (Alliance A091401): two open-label, non-comparative, randomised, phase 2 trials. Lancet Oncol 2**018;**19(3):416-26 doi 10.1016/S1470-2045(18)30006-8.
51. Tawbi HA, Burgess M, Bolejack V, Van Tine BA, Schuetze SM, Hu J, *et al.* Pembrolizumab in advanced soft-tissue sarcoma and bone sarcoma (SARC028): a multicentre, two-cohort, single-arm, open-label, phase 2 trial. Lancet Oncol 2**017;**18(11):1493-501 doi 10.1016/S1470-2045(17)30624-1.

52. Pollack SM, He Q, Yearley JH, Emerson R, Vignali M, Zhang Y, *et al.* T-cell infiltration and clonality correlate with programmed cell death protein 1 and programmed death-ligand 1 expression in patients with soft tissue sarcomas. Cancer 2**017;**123(17):3291-304 doi 10.1002/cncr.30726.
53. Beard RE, Zheng Z, Lagisetty KH, Burns WR, Tran E, Hewitt SM, *et al.* Multiple chimeric antigen receptors successfully target chondroitin sulfate proteoglycan 4 in several different cancer histologies and cancer stem cells. J Immunother Cancer 2**014;**2:25 doi 10.1186/2051-1426-2-25.
54. Majzner RG, Theruvath JL, Nellan A, Heitzeneder S, Cui Y, Mount CW, *et al.* CAR T Cells Targeting B7-H3, a Pan-Cancer Antigen, Demonstrate Potent Preclinical Activity Against Pediatric Solid Tumors and Brain Tumors. Clin Cancer Res 2**019;**25(8):2560-74 doi 10.1158/1078-0432.CCR-18-0432.
55. Du H, Hirabayashi K, Ahn S, Kren NP, Montgomery SA, Wang X, *et al.* Antitumor Responses in the Absence of Toxicity in Solid Tumors by Targeting B7-H3 via Chimeric Antigen Receptor T Cells. Cancer Cell 2**019;**35(2):221-37.e8 doi 10.1016/j.ccell.2019.01.002.
56. Nishimura R, Baker J, Beilhack A, Zeiser R, Olson JA, Sega EI, *et al.* In vivo trafficking and survival of cytokine-induced killer cells resulting in minimal GVHD with retention of antitumor activity. Blood 2**008;**112(6):2563-74.
57. Franceschetti M, Pievani A, Borleri G, Vago L, Fleischhauer K, Golay J, *et al.* Cytokine-induced killer cells are terminally differentiated activated CD8 cytotoxic T-EMRA lymphocytes. Exp Hematol 2**009;**37(5):616-28 e2 doi S0301-472X(09)00031-9 [pii]10.1016/j.exphem.2009.01.010.

Figure Legends

Figure 1. CSPG4 is highly expressed in multiple STS histotypes.

CSPG4 mRNA expression in multiple STS histotypes (Leiomyosarcoma; Dedifferentiated Liposarcoma; Undifferentiated pleomorphic sarcoma (UPS), Malignant Fibrous Histiocytoma, High-Grade Spindle Cell Sarcoma; Myxofibrosarcoma; Malignant Peripheral Nerve Sheath Tumor; Synovial Sarcoma). CSPG4 expression in STS was comparable to that observed in melanoma. RNA-sequencing expression data were selected and downloaded from the cBioPortal of the TCGA Pan-Cancer Collections. RSEM expression values were plotted after Log2 transformation with 0.5 jittering on the x-axis, using Microsoft Excel®. **(A)**. CSPG4 expression was confirmed in patient-derived STS cell lines of various histologic types by flow cytometry. A representative flow-cytometry histogram is reported for each STS. The M14 melanoma cell line that lacks CSPG4 expression and normal keratinocytes were used for comparison. Isotype controls are shown in grey **(B)**. Grey histograms show the number of CSPG4 molecules expressed on the cell surface of various patient-derived STS cell lines quantified as the CSPG4-specific mAb-binding capacity (sABC) on a per cell basis **(C)**.

Abbreviations: CSPG4, Chondroitin Sulfate proteoglycan 4; STS, Soft Tissue Sarcoma.

Figure 2. CSPG4-CAR.CIK effectively and specifically target STS cells *in vitro*.

Patient-derived CSPG4-CAR.CIK efficiently targeted STS cells in vitro when using either HLA mismatched (10 samples) or matched CIK (2 samples). Specific cytotoxicity of CSPG4-CAR.CIK was significantly higher than that obtained with unmodified NTD.CIK. Tumor cell-specific cytotoxicity values from 29 experiments are reported (mean ± SEM) **(A)**. CSPG4-CAR.CIK retained their antitumor activity when challenged at very low E:T ratios (n=8) **(B)**. *In vitro* cytotoxic activity of control CD19-CAR.CIK against STS was comparable to that of unmodified NTD.CIK (n=5) **(C)**. CSPG4-CAR.CIK and paired unmodified NTD.CIK showed similar cytotoxic activity against the M14 control cell line that lacks CSPG4 expression (n=3) **(D)**. Both CSPG4-CAR.CIK and paired unmodified NTD.CIK did not lyse normal keratinocytes (n=5) **(E)**. CSPG4-CAR.CIK exhibited more intense killing of STS cells with high CSPG4 expression as compared with STS cells with low CPSG4 expression (n=7, * $P \leq 0.05$ by t-test) **(F)**. CSPG4-CAR.CIK, but not paired unmodified NTD.CIK, retained cytotoxic activity against a STS sample expressing CSPG4, but lacking NKG2D ligands (S061) (n=3; two-way ANOVA and Bonferroni's post-test analysis) **(G)**. STS cell growth assessed 48 hours following *in vitro* treatment was significantly delayed in STS exposed to CSPG4-CAR.CIK, as compared with unmodified NTD.CIK. The dashed line represents the control parallel growth of untreated STS cells (n=2, * $P \leq 0.05$ by unpaired t-test) **(H).** CSPG4-CAR.CIK displayed significant and superior STS killing activity compared to paired "non-cytokine-induced", but minimally activated with IL-2 (50U/ml) CAR.T expressing comparable membrane levels of CSPG4-specific CAR molecules (n=2, two-way ANOVA and Bonferroni's post-test analysis) **(I).**
All cytotoxicity assays were analyzed by two-way ANOVA and Bonferroni's post-test analysis; statistical significance is reported as * $P \leq 0.05$, ** $P \leq 0.01$, *** $P \leq 0.001$, and **** $P \leq 0.0001$; "n" refers to the number of separate experiments.

Abbreviations: CIK, Cytokine Induced Killer cells; CSPG4, Chondroitin Sulfate proteoglycan 4; CAR, Chimeric Antigen Receptor; NTD, Not Transduced; STS, Soft Tissue Sarcoma.

Figure 3. CSPG4-CAR.CIK effectively target STS cells in 3D spheroids.

Schematic showing the 3D assay to test the cytotoxic activity of CSPG4-CAR.CIK against GFP-expressing STS spheroids (green) **(A)**. CSPG4-CAR.CIK showed superior tumor elimination, as compared to paired unmodified NTD.CIK. Shown are representative microscope fluorescence images and surface plot images of GFP-

expressing STS spheroids (green) treated with CSPG4-CAR.CIK (up to 72 hours) and control CIK. Magnification: 10X; Scale bars: 100 µm **(B)**.

Abbreviations: CIK: Cytokine Induced Killer cells; CSPG4: Chondroitin Sulfate proteoglycan 4; CAR: Chimeric Antigen Receptor; NTD: Not Transduced; STS: Soft Tissue Sarcoma; GFP: Green Fluorescent Protein.

Figure 4. CSPG4-CAR.CIK infiltrate 3D STS spheroids.

CSPG4-CAR.CIK displayed cytolytic activity against 3D STS spheroids. Tumor cell elimination mediated by CSPG4-CAR.CIK was quantified by measuring GFP fluorescence loss overtime of S1 **(A)**, S5 **(B)** and S172 **(C)** spheroids (pixel) by fluorescence microscopy. Values are reported as means (±SEM) from three independent wells (2:1 E:T ratio). Results were analyzed by two-way ANOVA and Bonferroni's post-test analysis; statistical significance is reported as * $P \leq 0.05$, ** $P \leq 0.01$, *** $P \leq 0.001$, and **** $P \leq 0.0001$. Representative maximum intensity projections of confocal microscopy images for S5 **(D)** and S172 **(E)** spheroids (green) treated with unmodified PKH26-stained (red) NTD.CIK and CSPG4-CAR.CIK (2:1 E:T ratio). Confocal microscopy images taken 16 hours after co-incubating CIK and STS spheroids. 20X magnification and scale bars: 100 µm are shown. **(F)** CSPG4-CAR.CIK displayed superior infiltration within the STS spheroids (green) as compared with paired unmodified NTD.CIK (n=8, $P \leq 0.05$ by paired t-test). CSPG4-CAR.CIK density was determined as red fluorescent PKH26 area (μm^2).

Abbreviations: CIK: Cytokine Induced Killer cells; CSPG4: Chondroitin Sulfate Proteoglycan 4; CAR: Chimeric Antigen Receptor; NTD: Not Transduced; STS: Soft Tissue Sarcoma; GFP: Green Fluorescent Protein.

Figure 5. CSPG4-CAR.CIK penetrate Matrigel matrix toward the STS spheroids.

Schematic showing the Matrigel® based penetration assay. STS spheroids were embedded into Matrigel® domes and co-cultured with either PKH26-stained CSPG4-CAR.CIK or unmodified NTD.CIK at E:T ratios 10:1. Empty domes served as controls. Fluorescence microscope images were acquired at day 5 of co-culture **(A).** Representative imagines of CSPG4-CAR.CIK and unmodified NTD.CIK empty or STS spheroids embedded in Matrigel® domes are displayed. Dashed lines represent Matrigel® boundaries. Top panel includes bright field microscope images; bottom panel includes fluorescent images. Magnification: 4X; Scale bars: 100 µm **(B).** Summary showing that CSPG4-CAR.CIK displayed superior ability in penetrating Matrigel® domes as compared to paired NTD.CIK (n=5, $P \leq 0.01$ by paired t-test). CSPG4-CAR.CIK density was defined as the fluorescent PKH26 area (μm^2) **(C).**

Abbreviations: CIK: Cytokine Induced Killer cells; CSPG4: Chondroitin Sulfate Proteoglycan 4; CAR: Chimeric Antigen Receptor; NTD: Not Transduced; STS: Soft Tissue Sarcoma.

Figure 6. CSPG4-CAR.CIK are active against STS in xenograft models.

Schematic representation of the STS xenografts and treatment with CSPG4-CAR.CIK (red arrows) and NTD.CIK (blue arrows). Vehicle-treated mice were infused with PBS (grey arrows). CIK were infused intravenously ($1x10^6$ cells/infusion) twice a week for 2 weeks **(A).** Autologous CSPG4-CAR.CIK caused a significant delay of the growth of the S172 leiomyosarcoma (CSPG4=72% and CSPG4 density=262 molecule/cell) as compared to unmodified NTD.CIK or vehicle-treated mice (n=6; $p<0.05$) **(B).** Autologous CSPG4-CAR.CIK caused a significant delay of the growth of the HT1080 fibrosarcoma (CSPG4=23% and CSPG4 density=521 molecule/cell) as compared to unmodified NTD.CIK or vehicle-treated mice (n=3, $p<0.001$). **(C).** Autologous CSPG4-CAR.CIK effectively delayed the growth of S1 UPS (CSPG4=95% and CSPG4 density=499 molecule/cell) as compared with controls (n=3, $p<0.0001$). All results were analyzed by two-way ANOVA and the Bonferroni post-test; statistical significance is reported as * $P \leq 0.05$, ** $P \leq 0.01$, *** $P \leq 0.001$, and **** $P \leq 0.0001$.

(D). Tumor-homing of CSPG4-CAR.CIK and unmodified NTD.CIK was confirmed by IHC in explanted tumors using an anti-human CD3 antibody staining. Magnification: 40X; Scale bars: 50 µm **(E)**. Apoptotic tumor cells were visualized by detecting cleaved caspase 3 by IHC in explanted tumors **(F)**.

Abbreviations: CIK: Cytokine Induced Killer cells; CSPG4: Chondroitin Sulfate Proteoglycan 4; CAR: Chimeric Antigen Receptor; NTD: Not Transduced; NOD/SCID: Non-obese diabetic/severe combined immunodeficiency mice; NSG: NOD/SCID gamma mice.

Figure 1. CSPG4 is highly expressed in multiple STS histotypes

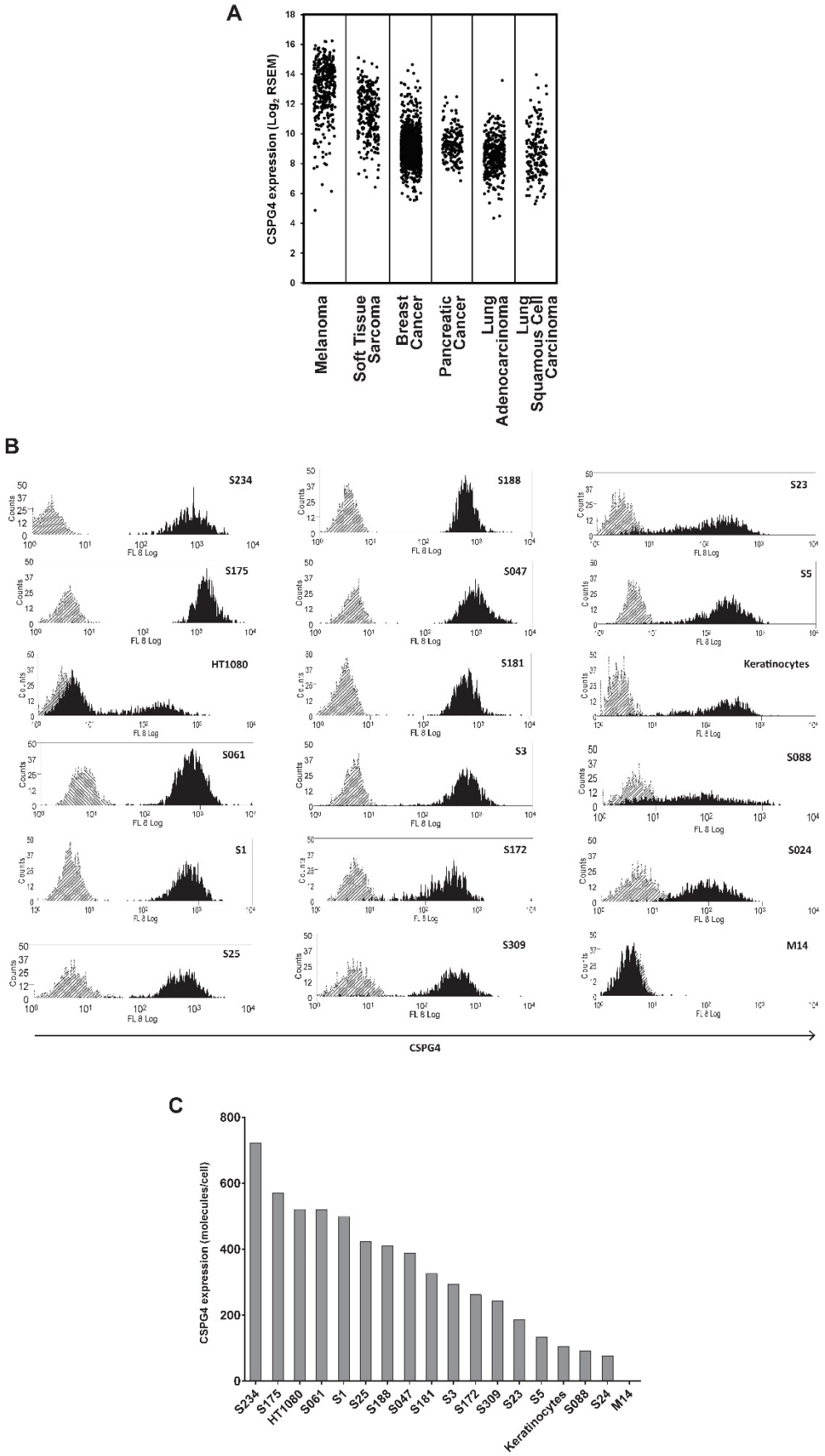

Figure 2. CSPG4-CAR.CIK effectively and specifically target STS cells *in vitro.*

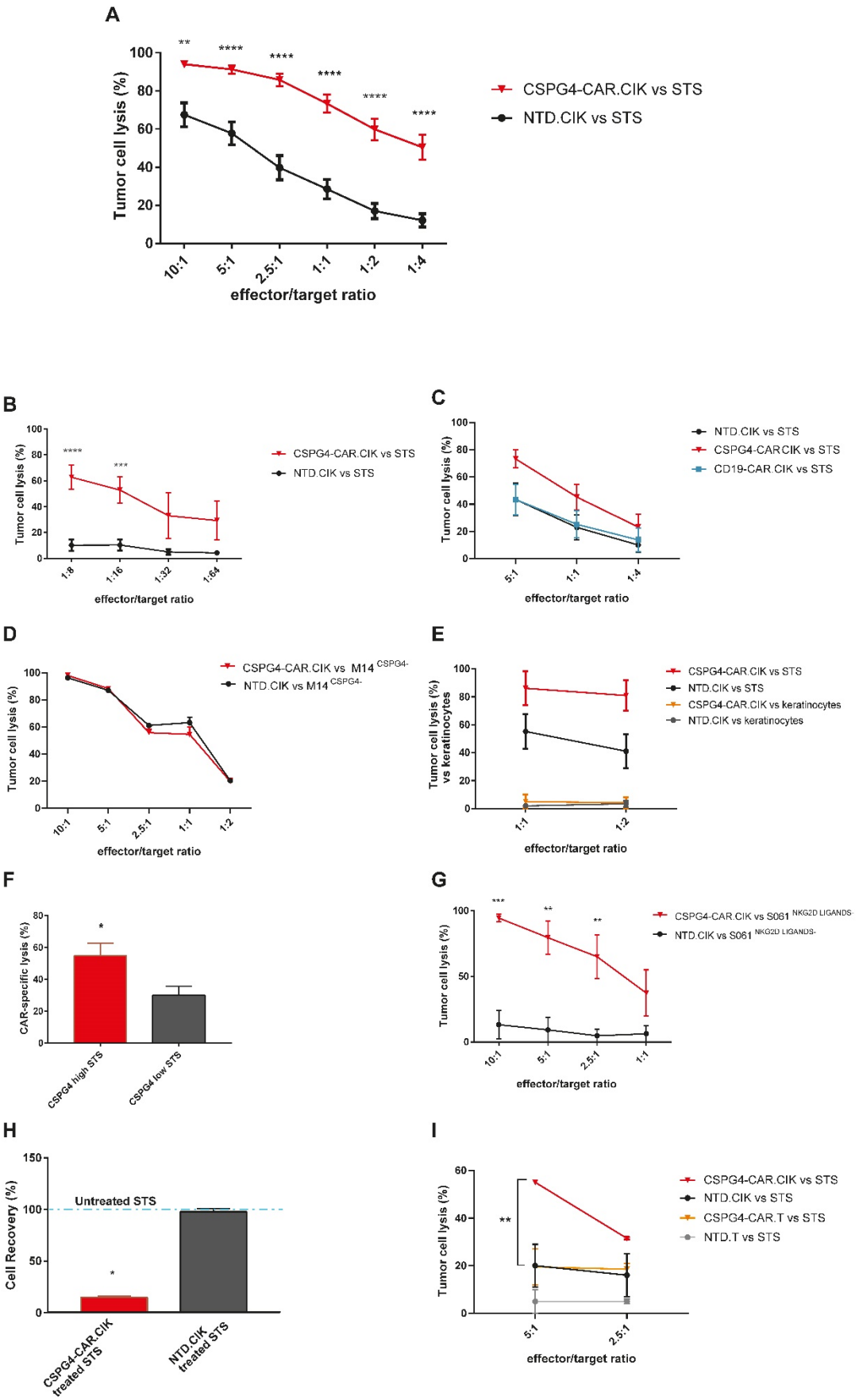

Author Manuscript Published OnlineFirst on September 8, 2020; DOI: 10.1158/1078-0432.CCR-20-0357
Author manuscripts have been peer reviewed and accepted for publication but have not yet been edited.

Figure 3. CSPG4-CAR.CIK effectively target STS cells in 3D spheroids.

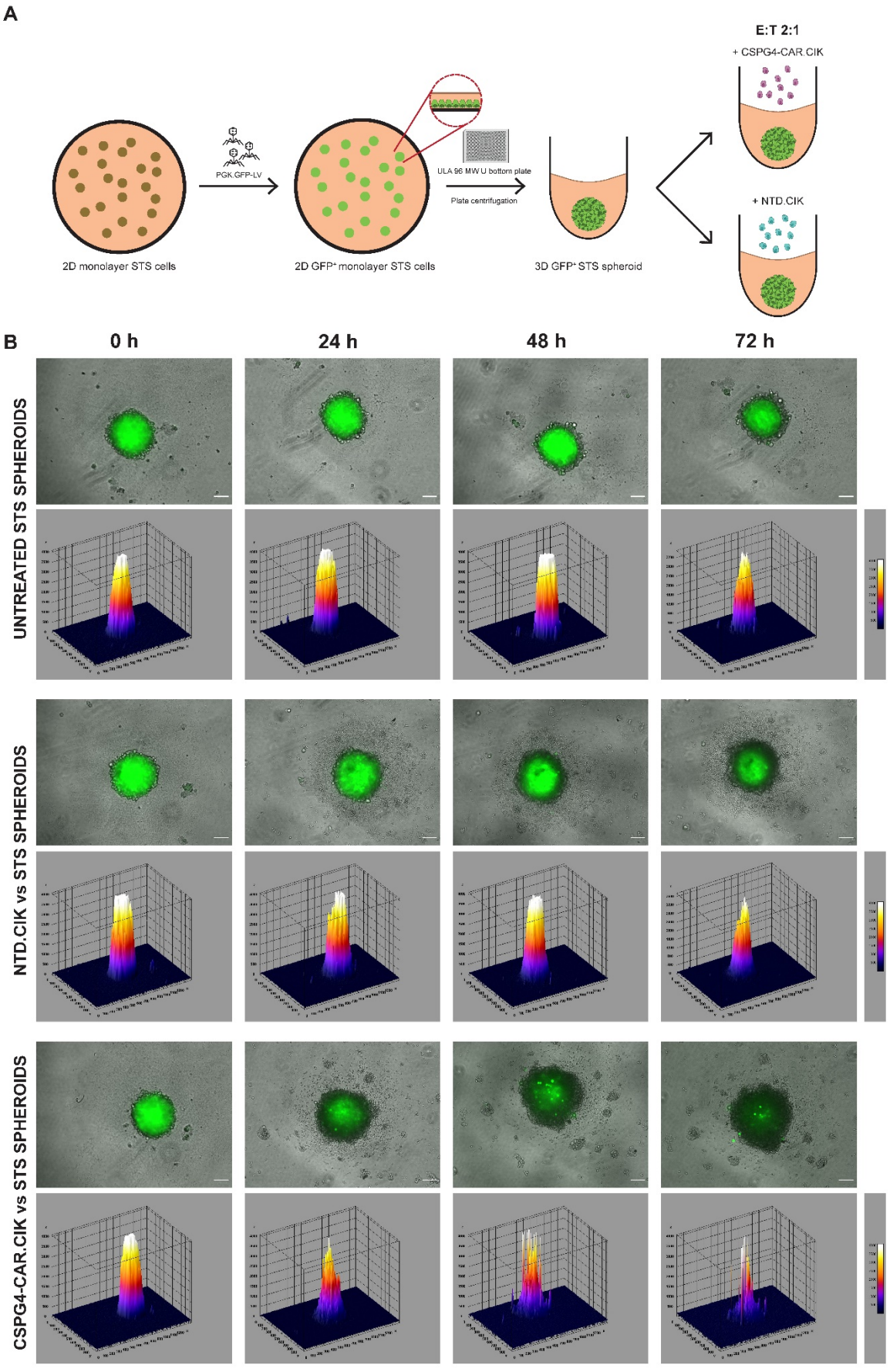

Figure 4. CSPG4-CAR.CIK infiltrate 3D STS spheroids.

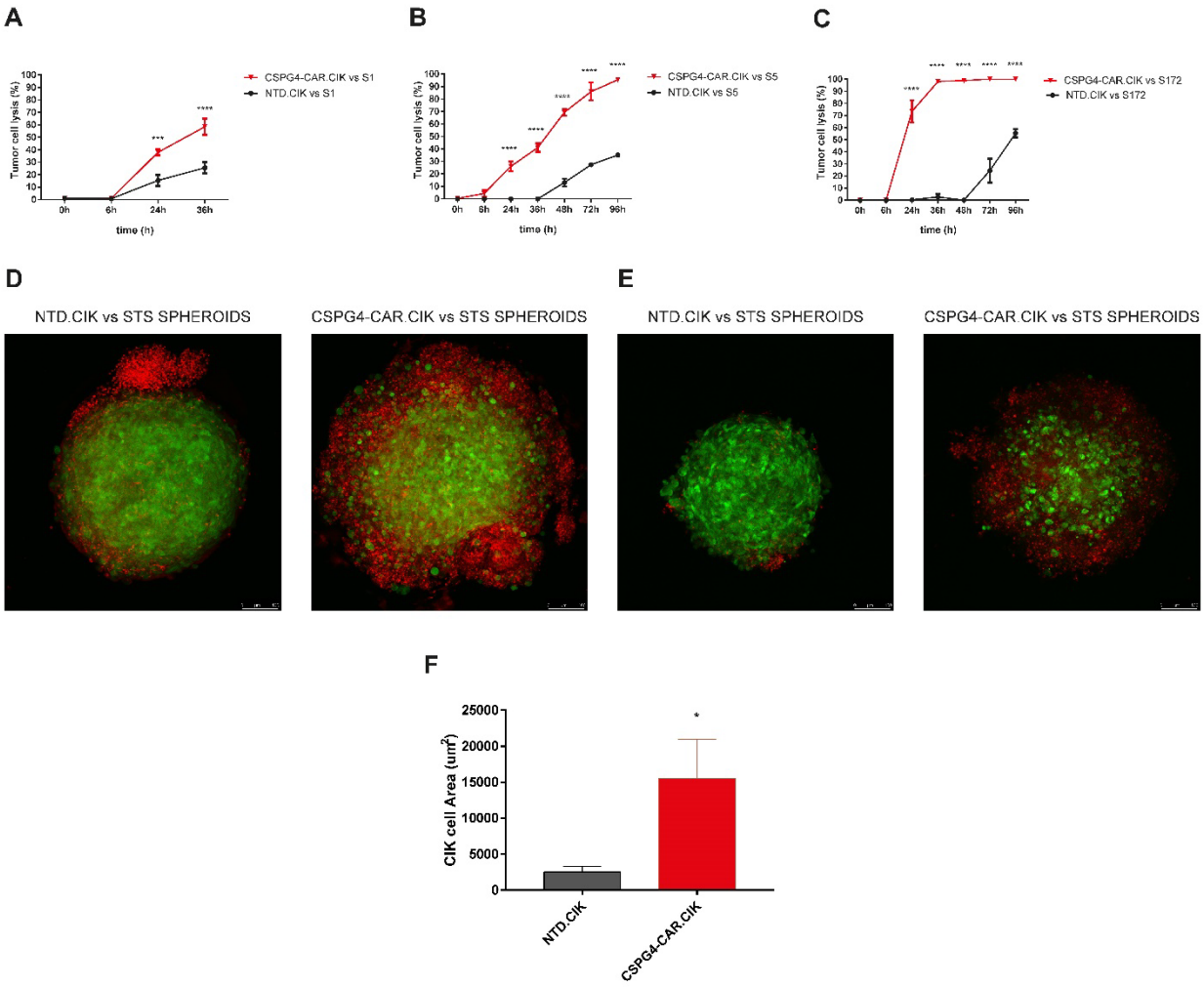

Author Manuscript Published OnlineFirst on September 8, 2020; DOI: 10.1158/1078-0432.CCR-20-0357
Author manuscripts have been peer reviewed and accepted for publication but have not yet been edited.

Figure 5. CSPG4-CAR.CIK penetrate Matrigel matrix toward the STS spheroids.

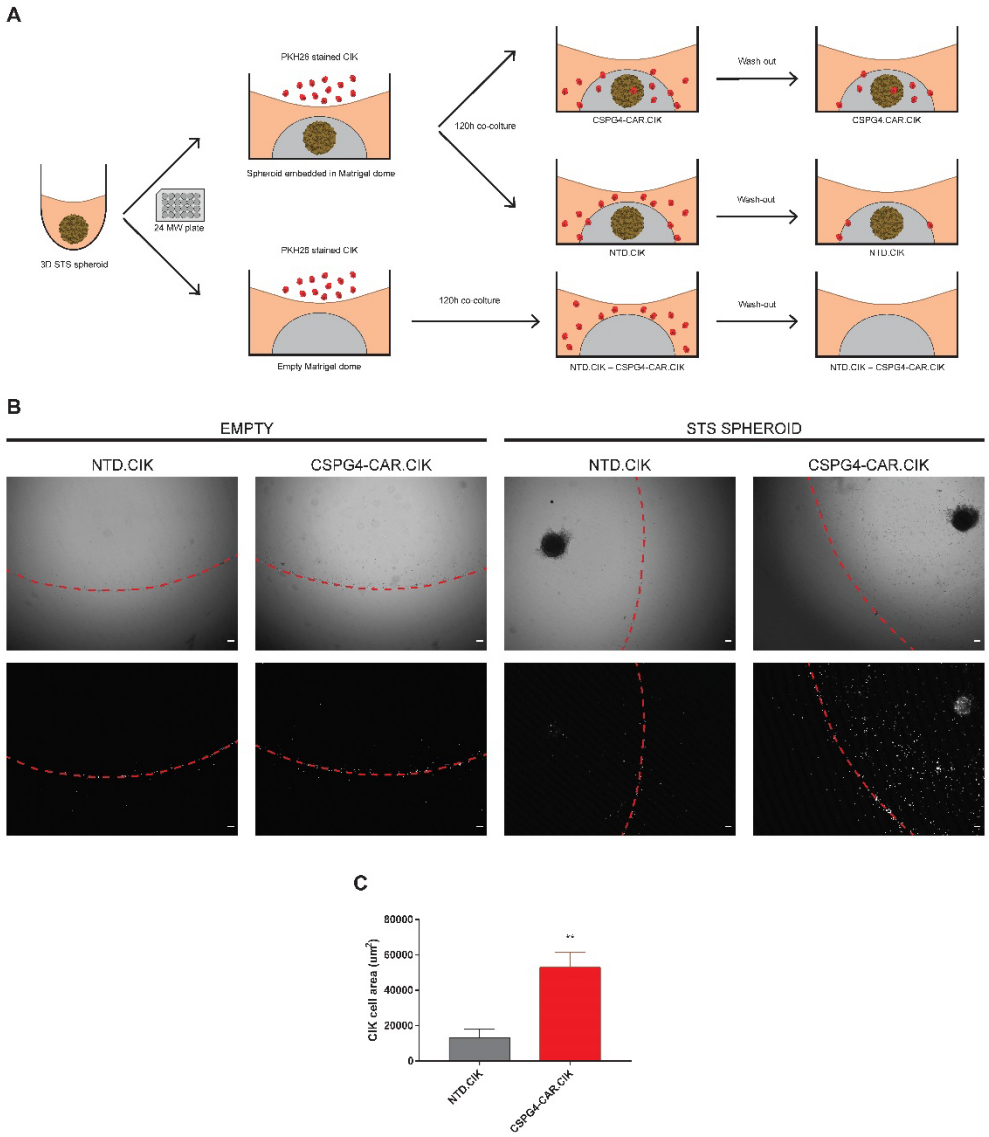

Figure 6. CSPG4-CAR.CIK are active against STS in xenograft models.

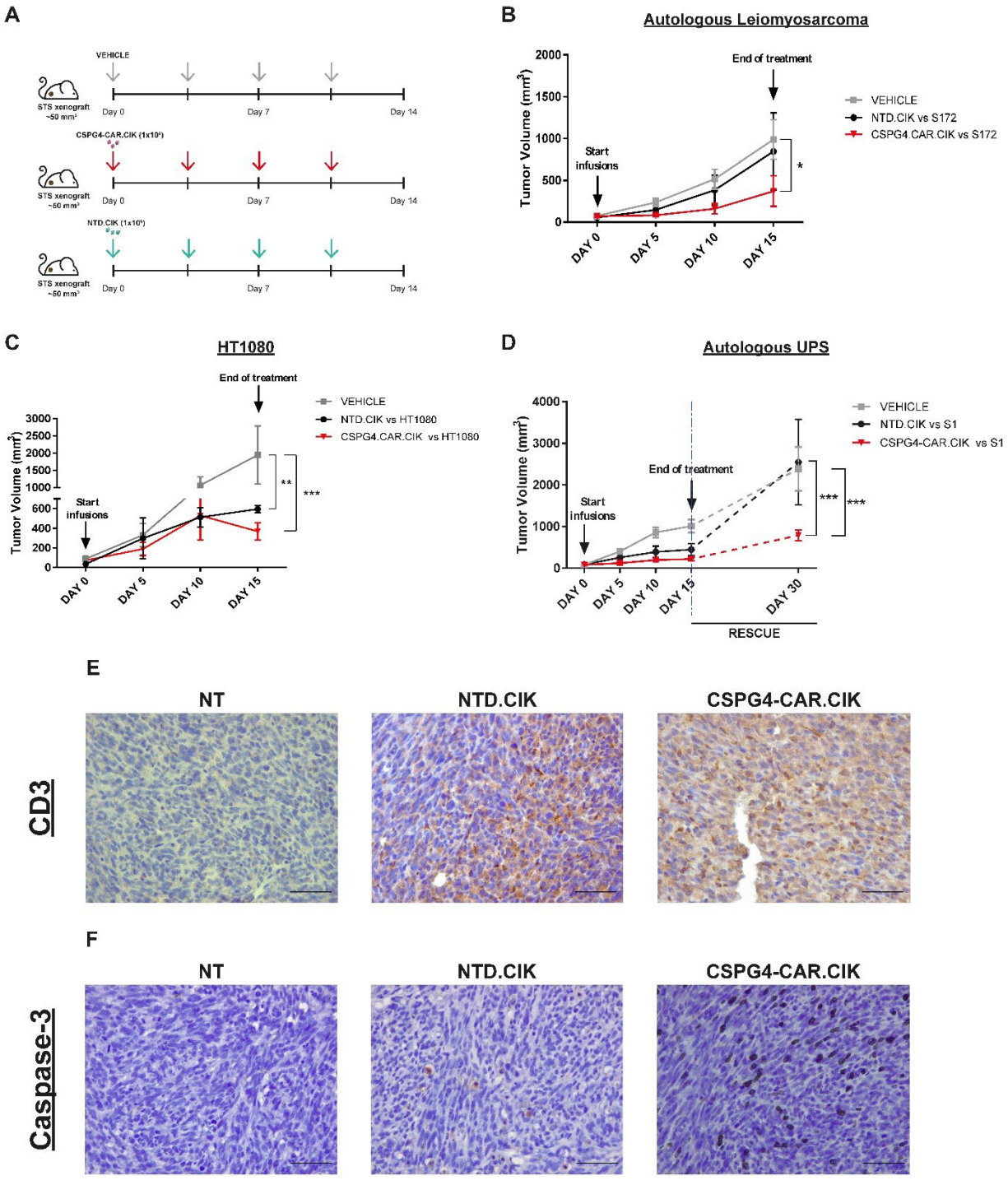

AACR American Association for Cancer Research

Clinical Cancer Research

CSPG4-specific CAR.CIK lymphocytes as a novel therapy for the treatment of multiple soft tissue sarcoma histotypes

Valeria Leuci, Chiara Donini, Giovanni Grignani, et al.

Clin Cancer Res Published OnlineFirst September 8, 2020.